

# Influence of Coagulation Factor X on *In Vitro* and *In Vivo* Gene Delivery by Adenovirus (Ad) 5, Ad35, and Chimeric Ad5/Ad35 Vectors

Jenny A Greig<sup>1</sup>, Suzanne MK Buckley<sup>2</sup>, Simon N Waddington<sup>2</sup>, Alan L Parker<sup>1</sup>, David Bhella<sup>3</sup>, Rebecca Pink<sup>3</sup>, Ahad A Rahim<sup>2</sup>, Takashi Morita<sup>4</sup>, Stuart A Nicklin<sup>1</sup>, John H McVey<sup>5</sup> and Andrew H Baker<sup>1</sup>

<sup>1</sup>British Heart Foundation Glasgow Cardiovascular Research Centre, University of Glasgow, Glasgow, UK; <sup>2</sup>Department of Haematology, Haemophilia Centre and Haemostasis Unit, Royal Free and University College Medical School, London, UK; <sup>3</sup>Medical Research Council Virology Unit, Institute of Virology, University of Glasgow, Glasgow, UK; <sup>4</sup>Department of Biochemistry, Meiji Pharmaceutical University, Tokyo, Japan; <sup>5</sup>Thrombosis Research Institute, London, UK

The binding of coagulation factor X (FX) to the hexon of adenovirus (Ad) 5 is pivotal for hepatocyte transduction. However, vectors based on Ad35, a subspecies B Ad, are in development for cancer gene therapy, as Ad35 utilizes CD46 (which is upregulated in many cancers) for transduction. We investigated whether interaction of Ad35 with FX influenced vector tropism using Ad5, Ad35, and Ad5/Ad35 chimeras: Ad5/fiber(f)35, Ad5/penton(p)35/f35, and Ad35/f5. Surface plasmon resonance (SPR) revealed that Ad35 and Ad35/f5 bound FX with approximately tenfold lower affinities than Ad5 hexon-containing viruses, and electron cryomicroscopy (cryo-EM) demonstrated a direct Ad35 hexon:FX interaction. The presence of physiological levels of FX significantly inhibited transduction of vectors containing Ad35 fibers (Ad5/f35, Ad5/p35/f35, and Ad35) in CD46-positive cells. Vectors were intravenously administered to CD46 transgenic mice in the presence and absence of FX-binding protein (X-bp), resulting in reduced liver accumulation for all vectors. Moreover, Ad5/f35 and Ad5/p35/f35 efficiently accumulated in the lung, whereas Ad5 demonstrated poor lung targeting. Additionally, X-bp significantly reduced lung genome accumulation for Ad5/f35 and Ad5/p35/f35, whereas Ad35 was significantly enhanced. In summary, vectors based on the full Ad35 serotype will be useful vectors for selective gene transfer via CD46 due to a weaker FX interaction compared to Ad5.

Received 9 April 2009; accepted 15 June 2009; published online 14 July 2009. doi:10.1038/mt.2009.152

## INTRODUCTION

Adenoviral vectors are under development for diverse gene delivery applications, especially cancer gene therapy and vaccination. The majority of these vectors are based on adenovirus (Ad) 5 (a subspecies C Ad), as it can be grown to high titers and is highly efficient at transducing nondividing cells. The effective use of Ad5

vectors is, however, severely hampered by a number of problems, including the broad prevalence of Ad5-specific neutralizing antibodies in the population,<sup>1–6</sup> the strong tropism of Ad5 for liver and spleen after intravenous administration,<sup>7–9</sup> the interaction of the Ad5 fiber with erythrocytes<sup>10–12</sup> and platelets,<sup>13,14</sup> and the overall toxicity profiles at high doses that have led to a well-publicized fatality.<sup>15</sup>

The fiber protein of Ad5 binds to the coxsackie virus and Ad receptor (CAR) as its primary attachment receptor to infect cells *in vitro*.<sup>16,17</sup> The interaction between fiber and CAR then promotes cell internalization through engagement of  $\alpha_v\beta_{3/5}$  integrins with the penton base.<sup>18</sup> Following intravascular administration in rodent models, Ad5 selectively accumulates within and transduces the liver.<sup>7,9</sup> Attempts to retarget this highly efficient mechanism, either by mutation of the Ad5 fiber or pseudotyping (replacement of the Ad5 fiber protein with a fiber from another Ad), have not been effective.<sup>19</sup> Moreover, mutations that ablate the Ad5:CAR interaction have no effect on hepatic uptake and transduction,<sup>20</sup> suggesting alternative pathways exist that dictate Ad tropism. Recently, we documented a direct, calcium-dependent interaction between Ad5 and the vitamin K-dependent blood coagulation factor X (FX).<sup>7</sup> Blockade of this interaction using warfarin, which prevents the maturation and secretion of functional vitamin K-dependent coagulation factors, substantially reduced liver transduction.<sup>7</sup> Infusion of FX rescued liver transduction unveiling a novel pathway that regulates Ad5-mediated gene transfer *in vivo*.<sup>7,8</sup> Electron cryomicroscopy (cryo-EM) determined that FX binds within cavities formed by trimeric hexon proteins and involves interaction with the Ad5 hexon hypervariable regions.<sup>9,21</sup> This interaction promotes the interaction of the Ad5–FX complex with cellular heparan sulfate proteoglycans (HSPGs) when bound to Ad5 (ref. 9). Therefore, utilization of HSPGs as receptors by the Ad5–FX complex, and not CAR, leads to liver transduction after systemic administration *in vivo*. Many previous studies to retarget the virus to alternate cells and organs have focused on fiber.<sup>22,23</sup> However, the role of hexon in dictating Ad biodistribution is now clear and is an increasingly relevant target for Ad modification.

**Correspondence:** Andrew H Baker, British Heart Foundation Glasgow Cardiovascular Research Centre, University of Glasgow, 126 University Place, Glasgow, G12 8TA, UK. E-mail: a.baker@clinmed.gla.ac.uk

Subspecies B Ad use the membrane protein CD46 as their high-affinity cellular receptor,<sup>24</sup> allowing more efficient transduction of both cancer and vascular cells in comparison to other subspecies.<sup>23,25</sup> Additionally, CD46 (which is usually present on all human nucleated cells) is upregulated in many cancers,<sup>26–28</sup> allowing the possibility to selectively target a large number of solid tumors. Studies have focused on chimeric vectors, where the fiber of different serotypes is “pseudotyped” onto the Ad5 capsid either through swapping of the knob domain<sup>24,29–31</sup> or the full-length fiber.<sup>25,26,30,32–38</sup> *In vitro*, this strategy is effective at improving delivery through CD46.<sup>26,32,33</sup> However, CD46 expression in rodents is restricted to the testes.<sup>39</sup> In nontransgenic mice, Ad5/f35 can selectively target liver metastases generated using human cancer cell lines, as cells express CD46 (ref. 40). Additionally, as some nonhuman primates express CD46 on erythrocytes, whereas humans do not, this has prevented their use as an *in vivo* model.<sup>41,42</sup> Therefore, it is appropriate to use mice transgenic for human CD46 that display a similar expression profile to humans.<sup>43</sup>

Although the interaction of FX with the Ad5 hexon has been reproduced,<sup>9,21,44</sup> the interaction of FX with Ad35 is controversial. In our previous work,<sup>9</sup> we reported that FX bound to Ad35 as demonstrated by surface plasmon resonance (SPR) and reported an equilibrium dissociation constant ( $K_D$ ) of  $5.2 \times 10^{-8}$  mol/l. Conversely, Kalyuzhnyi *et al.*<sup>21</sup> reported no interaction between Ad35 and FX by SPR. Based on this, and the importance of virus capsid design in gene therapeutics, we set out to fully define the interaction and effect of FX on Ad35 vectors *in vitro* and *in vivo*. To do this, we used chimeric vectors: the pseudotype Ad5/f35, which contains the hexon and penton of Ad5 with the Ad35 fiber, Ad5/p35/f35, which has the hexon of Ad5 and the penton and fiber of Ad35, and Ad35/f5, the reverse pseudotype.

Here, we demonstrate that FX binds to the Ad35 hexon, but the affinity is tenfold lower than that for the Ad5 hexon, and the chimeric vectors show affinities generally based on the parental hexon configuration. *In vitro*, we confirm that FX strongly enhances transduction by Ad5 whereas limiting transduction through CD46 for all viruses with an Ad35 fiber. *In vivo*, X-bp reduced liver virion accumulation for all viruses in CD46 transgenic mice. Preadministration of X-bp significantly reduced genome accumulation in the lung by Ad5/f35 and Ad5/p35/f35, but lung transduction by Ad35 was significantly enhanced in the presence of X-bp. Our study suggests that development of a gene therapy vector based on Ad35 and not a chimeric vector will provide the most efficient and selective targeting of CD46 *in vivo* after modifications to ablate the interaction between FX and Ad35.

## RESULTS

### Affinity analysis

The ability of the Ad5, Ad35, and the chimeric vectors to bind the blood coagulation FX was analyzed by SPR and compared to previous data characterizing the Ad5:FX interaction.<sup>9</sup> SPR analysis revealed that Ad5, Ad35, and the chimeric vectors bound to FX, and sensorgrams of the kinetic analysis for each vector are shown in **Figure 1**. The shape of the sensorgram was distinctly different depending on the capsid; thus, Ad5, Ad5/f35, and Ad5/p35/f35 had similar binding characteristics (**Figure 1a,c,e**), whereas Ad35 and Ad35/f5 shared different binding characteristics (**Figure 1b,d**), and this was reflected in the kinetic analysis. Vectors containing the Ad5 hexon (Ad5, Ad5/f35, and Ad5/p35/f35) fitted well to a 1:1 binding model with  $K_D$  of  $2.7 \times 10^{-9}$ ,  $1.9 \times 10^{-9}$ , and  $1.0 \times 10^{-9}$  mol/l, respectively, which is similar to our previously reported findings for Ad5 (ref. 9). It should be noted that the biotinylated Ad5/p35/f35 bound less FX than the other viruses. In contrast, vectors containing the Ad35 hexon (Ad35 and Ad35/f5) fitted poorly to a 1:1 binding model but fitted well to a heterogeneous ligand model with  $K_D$  of  $5.4 \times 10^{-8}$  and  $3.5 \times 10^{-9}$  mol/l for Ad35 and  $2.4 \times 10^{-8}$  and  $6.6 \times 10^{-9}$  mol/l for Ad35/f5. Therefore, both the Ad5 and Ad35 pseudotypes have FX-binding affinities akin to other vectors possessing the same serotype hexon (**Table 1**).

### Ad35 hexon binds to FX

The interaction between Ad35 and FX was further investigated by cryo-EM at 3.5 nm resolution. We observed that FX bound to the Ad35 hexon with a clear density in the center of the trimeric hexon proteins (**Figure 2**).

### Effect of FX on cell binding by Ad35 and the chimeric vectors in CHO-CD46 cells

First, we used the anti-CD46 antibody MEM258 to confirm that gene transfer was mediated by the membrane protein CD46 in the CHO-BC1 cell line (**Figure 3a**). The CHO-BC1 cell line stably expresses CD46, as the addition of MEM258 significantly reduced transduction by Ad35 by 22.6-fold compared to in the presence of IgG control antibody in CHO-BC1 cells as measured by quantification of luciferase transgene expression (**Figure 3a**). MEM258 does not affect transduction by Ad5 in either the CHO-BC1 or CHO-WTR cell line, which does not express CD46.

The addition of physiological levels of FX significantly increased binding of Ad5 to both CHO-BC1 and CHO-WTR cells, an effect inhibited by X-bp (**Figure 3b,c**). In the absence of FX, binding of Ad5/f35, Ad5/p35/f35, and Ad35 was considerably

**Table 1** Ad5, Ad35, and chimeric Ad5/Ad35 vectors bind FX

Vector	$k_{a1}$ (1/mol/l·s)	$k_{d1}$ (1/s)	$k_{D1}$ (mol/l)	$R_{max1}$ (RU)	$k_{a2}$ (1/mol/l·s)	$k_{d2}$ (1/s)	$k_{D2}$ (mol/l)	$R_{max2}$ (RU)
Ad5	$9.53 \times 10^5$	$2.5 \times 10^{-3}$	$2.7 \times 10^{-9}$	18.37				
Ad5/f35	$1.27 \times 10^6$	$2.4 \times 10^{-3}$	$1.9 \times 10^{-9}$	21.11				
Ad5/p35/f35	$1.90 \times 10^6$	$2.0 \times 10^{-4}$	$1.0 \times 10^{-9}$	1.90				
Ad35	$1.98 \times 10^5$	$1.1 \times 10^{-2}$	$5.4 \times 10^{-8}$	10.61	$2.09 \times 10^5$	$7.42 \times 10^{-4}$	$3.54 \times 10^{-9}$	4.08
Ad35/f5	$1.11 \times 10^{10}$	269.7	$2.4 \times 10^{-8}$	30.72	$2.29 \times 10^5$	$1.52 \times 10^{-3}$	$6.64 \times 10^{-9}$	22.39

Abbreviations: FX, factor X; RU, response units; SPR, surface plasmon resonance.

SPR kinetic analysis determined the calculated association rate ( $k_a$ ), dissociation rate ( $k_d$ ), and equilibrium dissociation constant ( $K_D$ ) values for each vector.

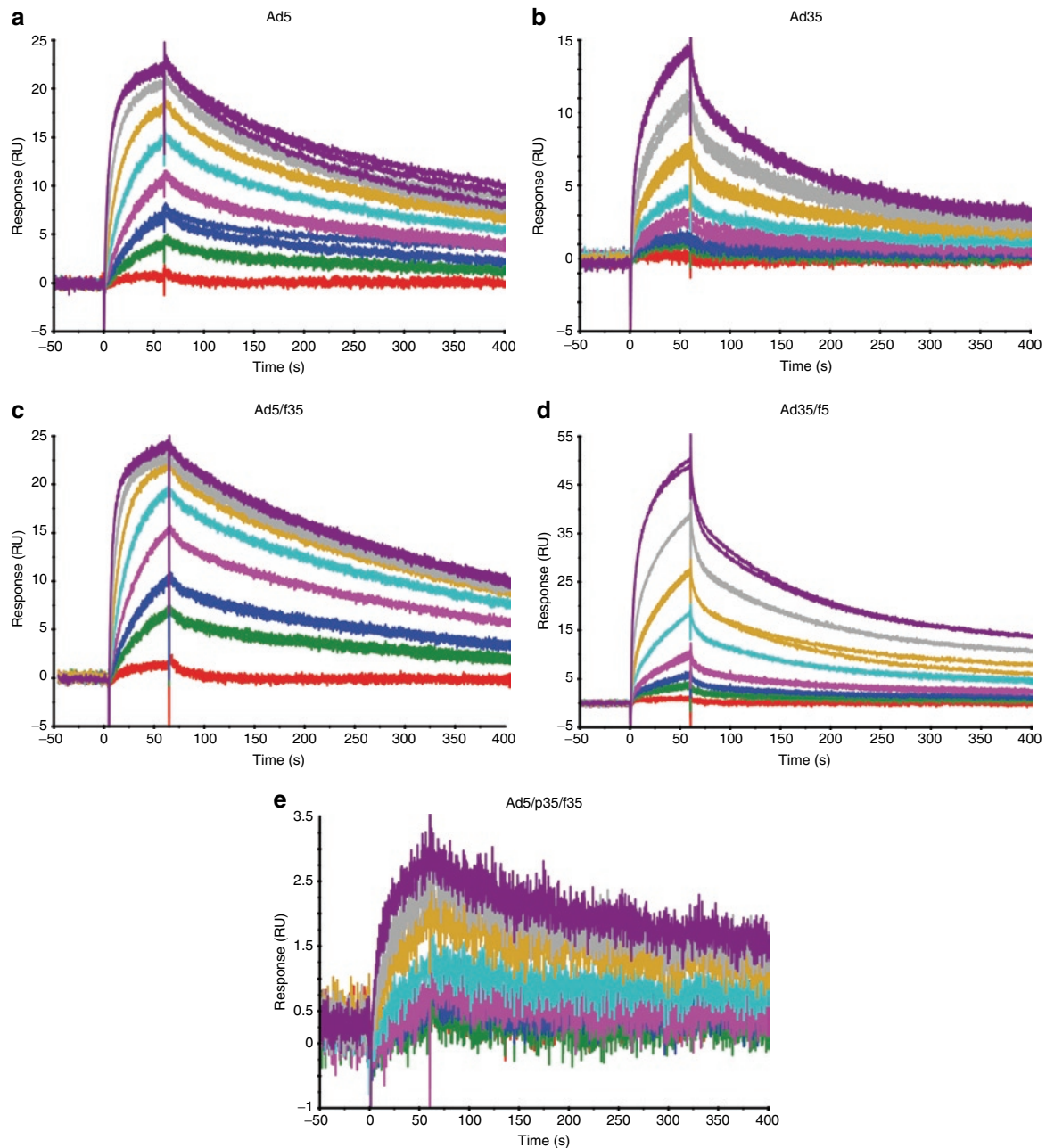


**Figure 1** Ad5, Ad35, and chimeric Ad5/Ad35 vectors bind FX. Representative SPR sensorgrams for (a) Ad5, (b) Ad35, pseudotype vectors, (c) Ad5/f35, (d) Ad35/f5, and (e) chimeric vector Ad5/p35/f35. All vectors bind FX as shown by an increase in response units (RU). FX, factor X.

higher in CHO-BC1 cells compared to binding in CHO-WTR cells as expected (Figure 3b,c). The addition of FX had no effect on CHO-BC1 cell binding mediated by Ad5/f35, Ad5/p35/f35, and Ad35 (Figure 3b) but enhanced binding of each in CHO-WTR cells (Figure 3c). Ad35/f5 showed a similar profile to Ad5 in both CHO-BC1 and CHO-WTR cells (Figure 3b,c). Taken together, these data suggest that FX can enhance cellular binding of vectors with the Ad5 fiber following interaction with the respective hexon protein and that this effect is inhibited fully by X-bp. Furthermore, in the presence of the Ad35 fiber (Ad5/f35, Ad5/p35/f35, and Ad35), the high-affinity interaction of the fiber with CD46 is not further enhanced by FX. However, in the absence

of this interaction (*i.e.*, in CHO-WTR cells), FX can enhance cell binding in a similar manner to that observed with Ad5.

#### Effect of FX on cell internalization by Ad35 and the chimeric vectors in CHO-CD46 cells

Previous reports have demonstrated differences in intracellular trafficking by vectors based on the subspecies B Ads.<sup>45,46</sup> Therefore, the level of cellular internalization mediated by the vectors was assessed through repetition of the binding experiment and with additional 1-hour incubation at 37°C and removal of cell surface-bound vector by washing with 0.2 mol/l glycine, pH 2.2. The addition of physiological levels of FX significantly enhanced cell

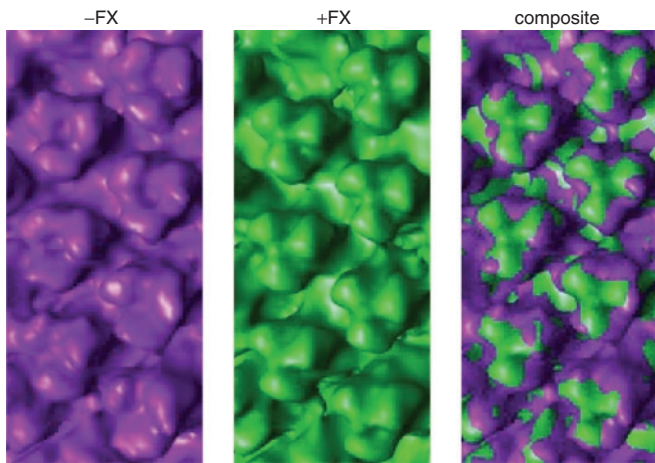


**Figure 2** FX binds to the Ad35 hexon. Cryo-electron microscopic reconstruction of Ad35 in the presence and absence of FX. Composite image shows FX bound within a cavity formed by Ad35 trimeric hexon proteins. FX, factor X.

entry by vectors containing the Ad5 fiber (Ad5 and Ad35/f5) in the CHO-BC1 cell line (**Figure 4a**). Additionally, FX significantly increased cell internalization by Ad35, indicating that FX and the resulting interaction with HSPGs can further enhance cell entry by Ad35 (**Figure 4a**). Cell internalization by all vectors was significantly enhanced by the addition of FX in CHO-WTR cells (**Figure 4b**). This was expected due to the absence of CD46 in the CHO-WTR cell line.

**FX limits cellular transduction by Ad35 and chimeric vectors containing the Ad35 fiber in CHO-CD46 cells**

In the presence of physiological levels of FX, the level of transgene expression mediated by Ad5 significantly increased 3.6-fold in CHO-BC1 cells and 38.6-fold in CHO-WTR cells and was entirely inhibited by X-bp (**Figure 5**). In the presence of FX, transduction by the Ad5/f35, Ad5/p35/f35, and Ad35 viruses in the CHO-BC1 cells was significantly inhibited by 2.7-, 1.9-, and 2.2-fold, respectively (**Figure 5a**). Levels of expression were substantially lower for all three viruses in CHO-WTR cells (**Figure 5b**). Taken together, these data suggest that FX limits postinternalization mechanism(s) that lead to cellular transduction by viruses containing the Ad35 fiber (*i.e.*, Ad5/f35, Ad5/p35/f35, and Ad35). Such a limitation is not observed for Ad5 with a strong potentiation of binding and transduction in the presence of FX. Ad35/f5 also showed a significant increase in transduction in the presence of FX, which was then inhibited by X-bp, but in both the CHO-BC1 and CHO-WTR cell lines, the degree of transduction produced was very low (**Figure 5**).

**Effect of FX on liver targeting and transduction by Ad35 and chimeric vectors *in vivo***

To assess the influence of FX interactions *in vivo*, we backcrossed an established CD46 transgenic line onto white MF1 mice (see Materials and Methods and **Supplementary Figure S1**). Mice were injected intravenously with  $5 \times 10^{10}$  virus particles/mouse in the absence or presence of a preinjection of X-bp 30 minutes beforehand. Luciferase transgene expression was visualized by whole-body bioluminescence imaging 48 hours after

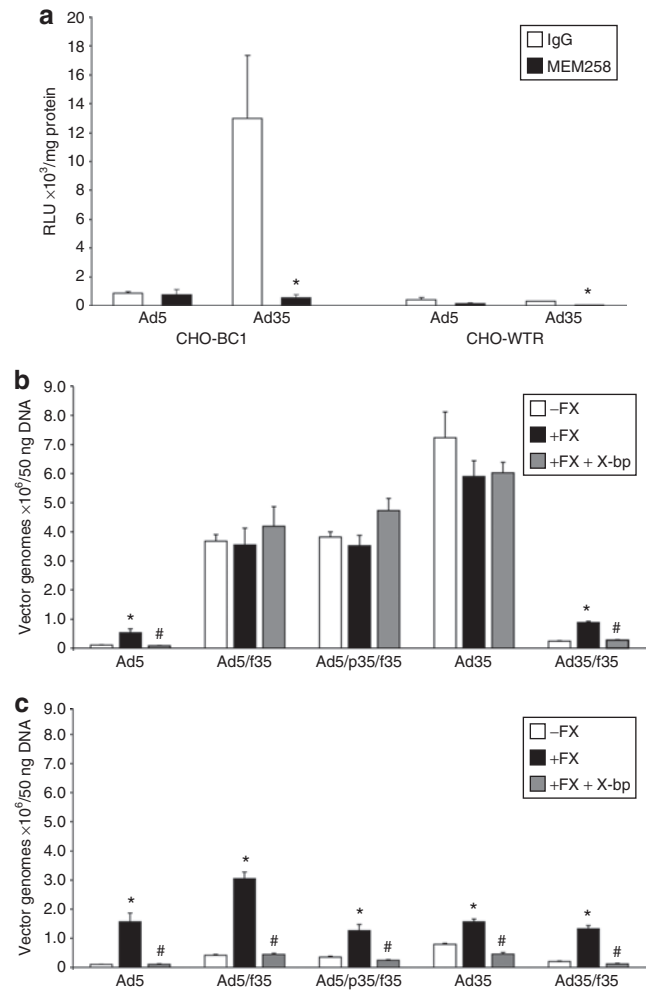


**Figure 3** Binding by Ad35 and chimeric Ad5/Ad35 vectors in CHO-CD46 cells. **(a)** CHO-BC1 cells express CD46, as transduction by Ad35 is significantly inhibited by anti-CD46 antibody MEM258 ( $*P < 0.05$  versus IgG control). **(b)** CHO-BC1 and **(c)** CHO-WTR (control cell line) cells were exposed to adenoviral vectors in the presence and absence of physiological FX levels and FX-binding protein, X-bp, for 1 hour at 4°C. Viral and total genomic DNA were extracted and the cell-bound adenovirus quantified by quantitative PCR. Error bars represent SEM ( $*P < 0.05$  versus absence of FX,  $#P < 0.05$  versus presence of FX). FX, factor X; RLU, relative light units.

administration (**Figure 6a**). Vector genomes were quantified by quantitative PCR of tissues 72 hours postadministration of the vectors (**Figure 6b,c**). Ad5 selectively targeted to the liver as expected, an effect that was significantly inhibited by X-bp. Liver virion levels for all other viruses were lower than that for Ad5 and were all significantly reduced further by X-bp (**Figure 6b**). This suggests that FX binding to both Ad5 and Ad35 hexon mediates liver accumulation and that this can be, at least partially, reduced by inhibition of the virus:FX interaction by X-bp.

**Effect of FX on *in vivo* lung transduction by Ad35 and the chimeric vectors**

It has previously been reported that vectors containing the Ad35 fiber possess the capacity to transduce the lungs of CD46 transgenic mice.<sup>43,47</sup> *In vivo* bioluminescent imaging confirmed this

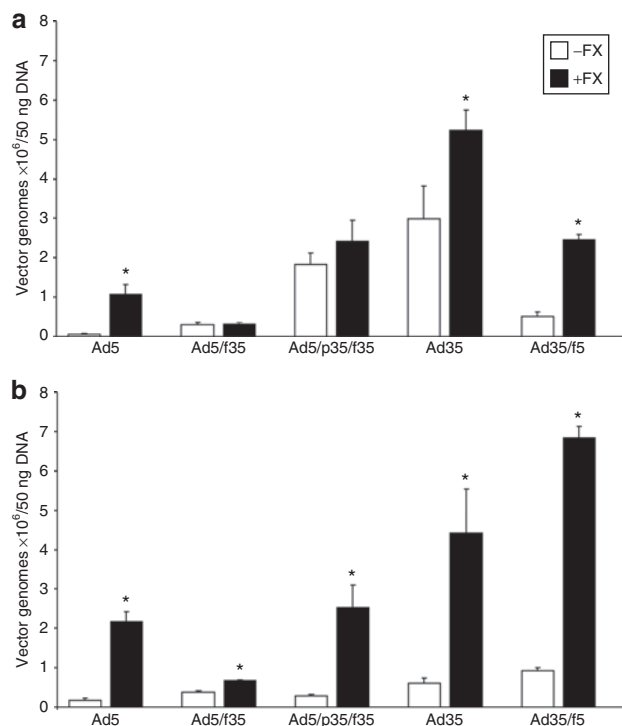


**Figure 4** Internalization by Ad35 and chimeric Ad5/Ad35 vectors in CHO-CD46 cells. **(a)** CHO-BC1 and **(b)** CHO-WTR cells were exposed to adenoviral vectors in the presence and absence of physiological FX levels for 1 hour at 4°C, followed by 1 hour at 37°C. After washing with 0.2 mol/l glycine, pH 2.2 to remove cell surface-bound vectors, viral and total genomic DNA were extracted and adenovirus quantified by quantitative PCR. Error bars represent SEM ( $*P < 0.05$  versus absence of FX). FX, factor X.

finding (Figure 6a). In the presence or absence of X-bp, Ad5 showed low-level vector accumulation in the lung (Figure 6c) and no luciferase activity (data not shown). This was also the case for Ad35/f5, which showed negligible vector accumulation in the lung (Figure 6c). In contrast, vectors with an Ad5 fiber, Ad5/f35, and Ad5/p35/f35 exhibited significantly higher levels of lung vector accumulation compared to Ad5 with  $5.6 \times 10^5$  and  $5.7 \times 10^5$  vector genomes/50 ng of total DNA isolated, respectively (Figure 6c). Preadministration of X-bp significantly reduced genome accumulation in the lung by Ad5/f35 and Ad5/p35/f35 1.9- and 6.6-fold, respectively, suggesting FX enhances vector accumulation in the lung mediated by these vectors, potentially via additive effects of CD46:Ad35 fiber interactions and the high-affinity Ad5:FX:HSPG interaction. Lung accumulation for Ad35 was lower than Ad5/f35 and Ad5/p35/f35, and modestly but significantly enhanced by X-bp. Levels of transgene expression were modest, yet visible and selective for the lung (Figure 6a). This suggests that Ad35 is efficient at utilizing CD46 for delivery *in vivo* and that targeting is most efficient and selective when FX binding is ablated by X-bp. Additionally, calculation of the lung:liver ratio of vector genome accumulation demonstrated that the addition of X-bp had no effect on retargeting Ad5/f35, as although the levels of vector accumulation in both the liver and lung are significantly reduced, the ratio of vector genomes present in these organs remains the same (Figure 6d). Ad5/p35/f35 had a reduced lung:liver ratio in

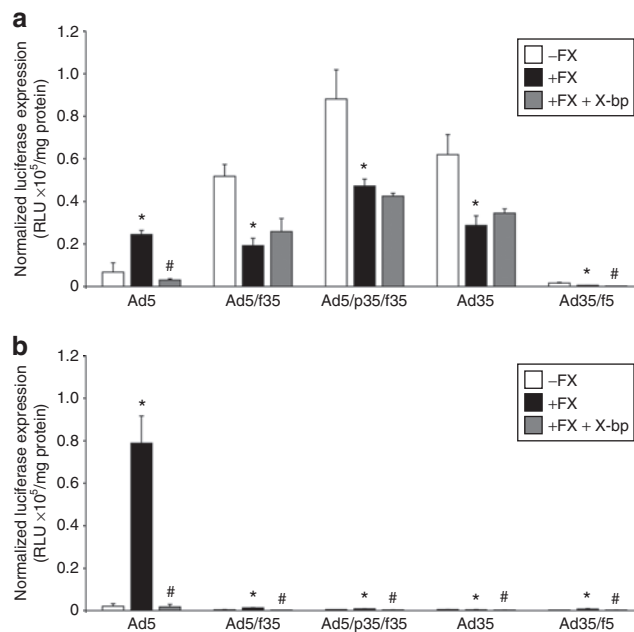


**Figure 5** Transduction by Ad35 and chimeric Ad5/Ad35 vectors in CHO-CD46 cells. **(a)** CHO-BC1 and **(b)** CHO-WTR cells were exposed to adenoviral vectors in the presence and absence of physiological levels of FX and FX-binding protein, X-bp, for 3 hours at 37°C. Luciferase expression was quantified at 72 hours postinfection and normalized to total protein content. Error bars represent SEM ( $*P < 0.05$  versus absence of FX,  $\#P < 0.05$  versus presence of FX). FX, factor X. RLU, relative light units.

the presence of X-bp indicating some level of retargeting through FX. Importantly, Ad35 had an increased lung:liver ratio in the presence of X-bp indicating retargeting of this vector to the lung after the addition of X-bp. The vectors possessing an Ad5 fiber (Ad5 and Ad35/f5) both had a very low lung:liver ratio further emphasizing the degree of liver targeting possessed by these vectors (Figure 6d).

## DISCUSSION

In this study, we have addressed the importance of coagulation factor binding on Ad5, Ad35, and chimeric Ad5/Ad35 vectors. We used a variety of capsid configurations to dissect the importance of FX. We have shown that the Ad35 hexon interacts directly with FX in a similar manner to Ad5 as evidenced by cryo-EM and SPR. Binding of FX to Ad35 showed two-component binding unlike Ad5. This difference was also seen in the pseudotyped viruses with Ad35/f5 and Ad5/f35 showing two- and single-component binding, respectively. Therefore, Ad35 and Ad35/f5 appear to have two binding sites for FX, the most abundant has a much faster dissociation leading to a substantially lower overall affinity in comparison to Ad5 and Ad5/f35. The affinity of FX interactions is dependent on the hexon with Ad5 hexon-containing viruses demonstrating higher affinity for FX ( $K_D$  values  $>10^9$ ) and Ad35 hexon-containing viruses show lower affinities (approximately tenfold lower than Ad5). In all cases, the FX-mediated effects are inhibited by the high-affinity FX Gla domain-binding protein X-bp. *In vivo*, liver virion DNA levels were variable across viruses but always sensitive to X-bp indicating that FX binding is an important feature in mediating liver uptake of Ad5- and Ad35-based vectors. In the

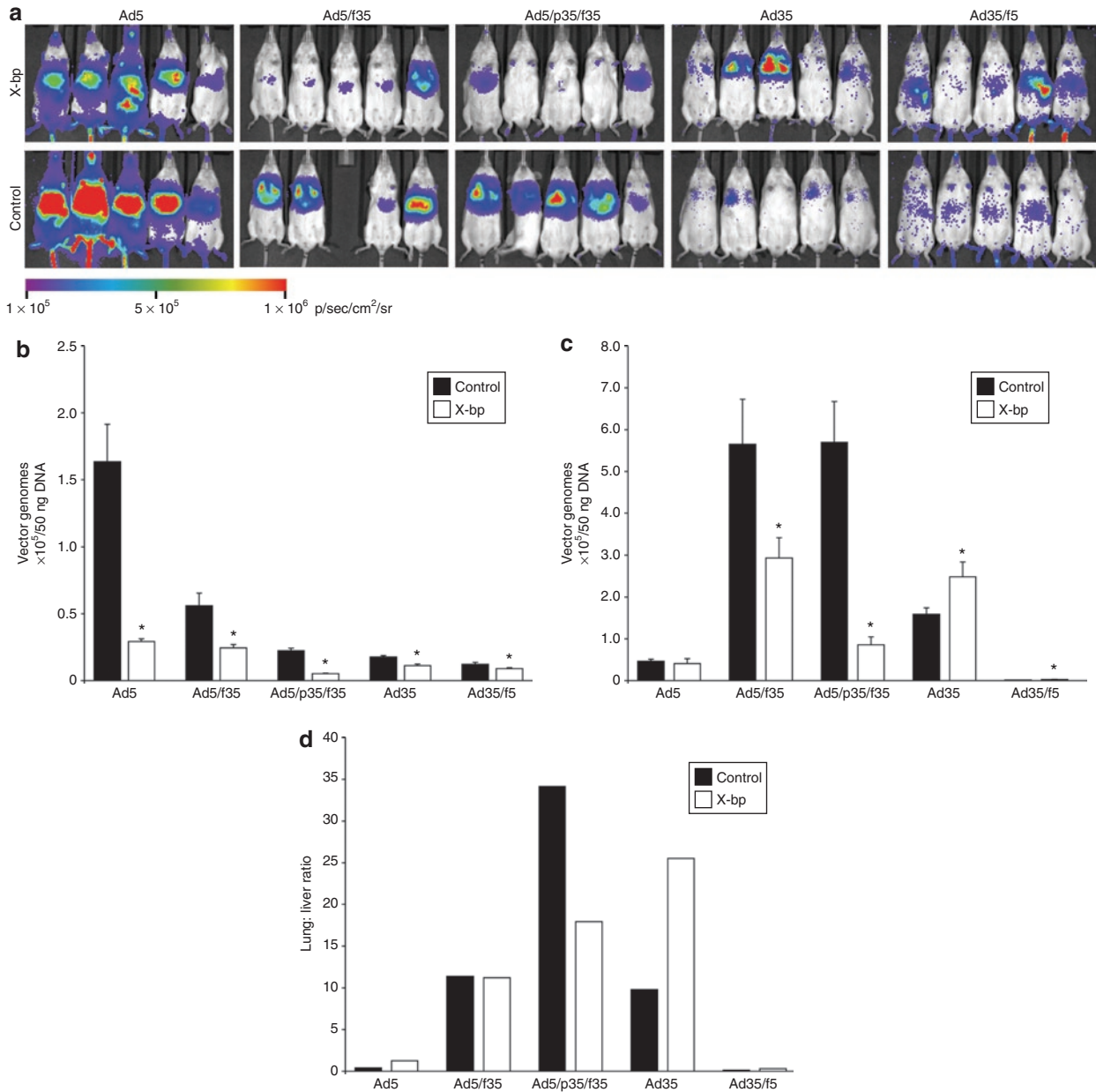


**Figure 6** Effect of FX on *in vivo* transduction by Ad35 and chimeric Ad5/Ad35 vectors. **(a)** Luciferase expression visualized by whole-body bioluminescence imaging 48 hours after systemic administration of  $5 \times 10^{10}$  virus particles/mouse into CD46 transgenic mice in the presence or absence of a preinjection of FX-binding protein, X-bp, 30 minutes before administration of the vector. Quantitative PCR on samples taken 72 hours post-administration of vectors in the presence or absence of X-bp preinjection 30 minutes before administration of the vector to determine the level of vector targeting to the **(b)** liver and **(c)** lung. Error bars represent SEM (\* $P < 0.05$  versus control). **(d)** Lung:liver ratio of vector genome accumulation/50 ng DNA. FX, factor X.

lung, accumulation of vector and resulting transgene expression showed a clear difference and was highly dependent on the hexon configuration present. Ad5 hexon-containing vectors have significantly reduced vector accumulation and transduction in the presence of X-bp, whereas the Ad35 hexon-containing vectors were significantly enhanced after the addition of X-bp.

Contrary to previous reports from other laboratories<sup>21</sup> but consistent with our previous findings,<sup>9</sup> we show that FX binds to Ad35. Kalyuzhniy *et al.*<sup>21</sup> used SPR to determine the affinity of the FX interaction with several human Ad serotypes and reported that

Ad35 does not bind to FX. Here, we have shown by SPR that the Ad35–FX interaction fitted well to a heterogeneous ligand model with  $K_D$  of  $5.4 \times 10^{-8}$  mol/l and  $3.5 \times 10^{-9}$  mol/l and further by cryo-EM that, like Ad5, binding is via the hexon protein with FX density in the center of the trimeric hexon proteins. It remains to be determined whether Ad35 hypervariable regions and specific loops mediate this interaction.

*In vitro*, the presence of FX has no effect on the degree of binding by those vectors possessing the Ad35 fiber in CHO-CD46 cells due to the high-affinity interaction between this fiber

and its primary cellular receptor, the membrane protein CD46. However, in the CHO-WTR cell line, FX significantly increased binding by all vectors, as no CD46 is expressed on this cell line and the presence of FX can facilitate increased binding through HSPGs. Cell internalization by Ad5, Ad35, and Ad35/f5 is significantly enhanced by the presence of FX in CHO-BC1 cells and for all vectors in the CHO-WTR cell line. This indicates that FX has the potential to increase cell entry by interaction of the vectors with HSPGs, in addition to the interaction with their cell surface receptors. *In vitro*, the interaction with FX also limits transduction through CD46 in the CHO-BC1 cell line by up to 2.7-fold, which can be reversed by the addition of X-bp. However, in the CHO-WTR cells, the addition of FX enhances transduction by Ad35 and the chimeric vectors up to 3.3-fold.

The findings *in vitro* indicate the complexity of the FX interaction, as the presence of FX can change the way in which binding, internalization, and trafficking by the vectors possessing the Ad35 fiber could possibly occur. In the absence of FX, vectors with an Ad35 fiber bind to CD46 that allows internalization of the vectors. The intracellular trafficking pathways of the subspecies B Ads have been previously studied.<sup>45,46</sup> Despite high levels of binding to cells, our data suggest that pseudotyped or full serotype subspecies B Ads take significantly longer than Ad5 to reach the nucleus of the cell despite no obvious difference in internalization kinetics.<sup>45</sup> Subspecies B Ads remain in late endosomes or lysosomes for long periods after infection and this can lead to recycling of the vectors to the cell surface resulting in reduced transduction by these vectors.<sup>46</sup> In contrast, Ad5 quickly escapes endosomes after internalization allowing efficient transduction. Addition of FX causes vectors containing the Ad35 hexon to switch from the use of two transduction pathways (high-affinity CD46 and low-affinity HSPG interaction<sup>48</sup>) to three pathways (CD46 and high- and low-affinity HSPG pathways).<sup>9</sup> Therefore, as addition of FX inhibits transduction by Ad35 hexon-containing vectors, this could be due to a hindrance in intracellular trafficking after internalization through the HSPG pathway. Taken together, and in context with the CHO-BC1 data, this suggests that the absolute levels of CAR, CD46, and HSPGs on the surface of target cells define the importance of FX in modulating cell binding and transduction mediated by Ad5, Ad35, and chimeric viruses.

Ad35 fiber-containing vectors, which use CD46 as their cellular receptor, are becoming increasingly popular as gene therapy agents for use in cell types, for example, cancer and vascular cells, which are relatively refractory to infection by Ad5, the most commonly used gene therapy vector. Ad5/f35 and Ad5/p35/f35, which both contain the Ad35 fiber, have significantly reduced liver transduction compared to Ad5. The high affinity of the Ad35 fiber for CD46 partially overcomes the Ad5 hexon:FX interaction, as the level of lung transduction in the animals administered with the chimeric vectors is significantly higher compared to Ad5. Determination of the lung:liver ratio for Ad5/f35 and Ad5/p35/f35 found that preadministration of X-bp had no effect on retargeting Ad5/f35, as the lung:liver ratio remained constant. However, the lung:liver ratio for Ad5/p35/f35 was significantly reduced in the presence of X-bp indicating retargeting away from the lung. Therefore, Ad5/f35 and Ad5/p35/f35 demonstrated the highest levels of selective lung targeting in the presence of FX, highlighting them as good

candidates for development as gene therapy vectors. However, as both Ad5/f35 and Ad5/p35/f35 possess the Ad5 hexon, these vectors will be susceptible to anti-Ad5 antibodies that are present in a high percentage of the population.<sup>1-6</sup> The resulting neutralization of these vectors *in vivo* might lead to very low levels of transduction after systemic administration and hinder their use as gene therapy vectors.

*In vivo*, Ad35 had an increased lung:liver ratio in the presence of X-bp indicating accumulation of this vector in the lung after the removal of the FX interaction. In conclusion, this study taken together with the low seroprevalence of Ad35 suggests that development of a vector based on Ad35 that had been modified to ablate the interaction with FX would be a highly useful tool to selectively target either endogenous CD46 expression in tissue or in pathological situations where CD46 is upregulated (such as in tumors) *in vivo* by intravascular administration.

## MATERIALS AND METHODS

**Analysis of FX binding to vectors.** SPR analysis was performed using a Biacore T100 (GE Healthcare, Little Chalfont, UK) as described.<sup>7</sup> Virus was biotinylated using sulfo-NHS-LC-biotin (Pierce, Rockford, IL) according to the manufacturer's instructions. Virus was covalently immobilized onto the flow cell of a streptavidin biosensor chip (SA; GE Healthcare) according to the manufacturer's instructions. FX in 10 mmol/l 4-(2-hydroxyethyl)-1-piperazineethanesulfonic acid pH 7.4; 150 mmol/l NaCl; 5 mmol/l CaCl<sub>2</sub>; 0.005% Tween 20 was passed over the chip at a flow rate of 30 µl/minute. Sensor chips were regenerated between FX application by injection of 10 mmol/l 4-(2-hydroxyethyl)-1-piperazineethanesulfonic acid pH 7.4; 150 mmol/l NaCl; 3 mmol/l EDTA; 0.005% Tween 20. Kinetic analysis was performed in triplicate using FX concentrations in the range of 108 to 0.05 µg/ml and analyzed using Biacore T100 evaluation software using either a 1:1 or heterogeneous ligand model.

**In vitro experiments.** Ads were propagated in 293 cells.<sup>7</sup> CHO-BC1 and CHO-WTR cells were maintained in Dulbecco's modified Eagle's medium/F-12 media (media and all supplements obtained from Invitrogen, Carlsbad, CA) supplemented with 10% fetal calf serum (PAA Laboratories, Yeovil, UK), 2 mmol/l L-glutamine, 1% penicillin, 100 µg/ml streptomycin, and 500 µg/ml Geneticin (G-418). For transgene expression, 4 × 10<sup>4</sup> cells/well were plated into 96-well plates and transferred to serum-free media ± 8 µg/ml FX (1 IU/ml; Cambridge Bioscience, Cambridge, UK). Virus was added at 1,000 virus particles/cell for 3 hours at 37°C, when complete media was added until harvesting at 72 hours. For antibody experiments, either 1 µg/ml MEM258 mouse antihuman CD46 antibody (AbD Serotec, Oxford, UK) or 100 µg/ml mouse IgG1 control (Dako, Glostrup, Denmark) in serum-free media was added to the cells 30 minutes before addition of virus. To further study the effect of FX, we used the FX-binding protein, X-bp, which was isolated from the venom of *Deinagkistrodon acutus* (hundred-pace snake) and binds with high affinity to FX.<sup>49</sup> X-bp (15 µg/ml) was preincubated with FX for 30 minutes before adding to cells. Expression of luciferase transgene was quantified using Luciferase Assay System (Promega, Madison, WI) and a Wallac VICTOR2 (PerkinElmer Life and Analytical Sciences, Boston, MA). Recombinant luciferase (Promega) was used as a standard. Protein concentrations were quantified by bicinchoninic acid assay (Perbio Science, Cramlington, UK). All data are presented as relative light units per milligram of protein. Cell-binding experiments were performed in 24-well plates with 2 × 10<sup>5</sup> cells/well, and in serum-free media ± FX, X-bp at 4°C for 1 hour using 1,000 virus particles/cell. For vector internalization experiments, cells were incubated at 37°C for 1 hour before a glycine wash (0.2 mol/l glycine, pH 2.2) for 10 minutes on ice, which was neutralized with 1 mol/l Tris, pH 8. Viral and total genomic DNA was isolated using QIAamp DNA

Mini Kit (Qiagen, Crawley, UK) and quantified by NanoDrop (ND-1000 spectrophotometer; Labtech International, Ringmer, UK). Fifty nanograms of total DNA was subjected to quantitative PCR analysis using ABI PRISM 7900HT Sequence Detection System (Applied Biosystems, Warrington, UK) using the Power SYBR Green PCR Master Mix as described.<sup>7</sup> Total Ad genomes were calculated using the Sequence Detection System 2.3 software and a standard curve of  $10^2$ – $10^7$  Ad particles.

**Cryo-EM.** Ad35 virions were incubated in the presence of an approximate threefold excess of FX overnight at 4°C. Complexed and noncomplexed virus was prepared for cryo-EM as previously described.<sup>50</sup> Briefly, 5 µl of virus was loaded onto a freshly glow-discharged Quantifoil holey carbon support film (R2/2; Quantifoil Micro Tools, Jena, Germany), blotted and plunged into a bath of liquid nitrogen-cooled ethane slush. Vitrified specimens were imaged at low temperature in a JEOL 1200 EXII transmission electron microscope (JEOL, Tokyo, Japan) equipped with an Oxford Instruments CT3500 (Oxford Instruments, Abingdon, UK) cryo-transfer stage. Low-dose focal pair images were recorded at  $\times 30000$  magnification on Kodak SO163 film (Kodak, New York, NY). Three-dimensional image reconstruction was then calculated as previously described.<sup>9</sup>

**In vivo methods.** CD46 transgenic mice were generated by backcrossing an established CD46 transgenic line onto white MF1 mice and were used for all *in vivo* experiments. To test for the presence of the CD46 transgene, DNA was extracted from mouse ear clips using the rapid NaOH method. Briefly, 75 µl 25 mmol/l NaOH and 0.2 mmol/l EDTA were added to the ear clip and the solution was heated to 95°C for 10 minutes. An equal volume of 40 mmol/l Tris-HCl, pH 8.0 was then added and 4 µl DNA was used in each 20 µl PCR reaction. Presence of the CD46 transgene was detected using the following primers and conditions; 5'-GCCTGTGAGGAGCCACCA-3' and 3'-CGTCATCTGAGACAGGTAG-5', 35 cycles of 94°C for 60 seconds, 55°C for 60 seconds, 72°C for 60 seconds, 178 base pair product size. To detect expression of CD46, western blots were performed. Briefly, protein was extracted from tissue by homogenization in T-PER solution (Thermo Fisher Scientific, Waltham, MA). Total protein was quantified using a colorimetric assay (Bio-Rad, Hercules, CA) and measured by a plate reader fitted with a 595 nm filter. The concentrations were standardized and 40 mg per sample underwent nonreducing sodium dodecyl sulfate-10% polyacrylamide gel electrophoresis. The protein fractions were transferred to a polyvinylidene membrane and then blocked in 5% milk to prevent nonspecific binding. CD46 was detected with goat antihuman CD46 (1:1,000; R&D Systems, Minneapolis, MN), followed by incubation with anti-goat IgG antibody labeled with horseradish peroxidase (1:1,000; R&D Systems). The signal was detected using Pierce enhanced chemiluminescent substrate (Thermo Fisher Scientific). To detect membrane-localized CD46, 50 µl of peripheral blood was extracted via the tail vein from CD46 transgenic mice and control wild-type mice and mixed with 10 µl of 500 units/ml heparin to prevent coagulation. Membrane-localized CD46 was detected by addition of 0.25 µg of phycoerythrin-labeled antihuman CD46 antibody (eBioscience, San Diego, CA) and incubation at 4°C in the dark for 40 minutes. The cells were washed twice with phosphate-buffered saline containing 1% bovine serum albumin (Sigma-Aldrich, Gillingham, UK) and resuspended in BD FACS lysing solution (BD Biosciences, San Jose, CA) to remove red blood cells. The cells were washed using 1% bovine serum albumin in phosphate-buffered saline and resuspended and fixed in a 1% paraformaldehyde solution. FACS analysis of the cells was achieved using the CyAn flow cytometer and Summit Software (Dako UK, Cambridgeshire, UK). The leukocyte and monocyte cell populations were gated for analysis (including control unstained cells) and plotted as an overlay histogram presenting fluorescence (log scale) against counts.

CD46 transgenic mice of 25–30 g were injected with  $5 \times 10^{10}$  virus particles/mouse. X-bp-treated animals were injected with 4.8 mg/kg X-bp 30 minutes before injection of Ad. Mice were subjected to whole-body bioluminescent quantification (IVIS Spectrum; Caliper Life Sciences)

48 hours post-Ad administration and were killed after 72 hours for tissue analysis. Tissue homogenates were produced from 25 mg tissue (10 mg spleen) using TissueLyser II (Qiagen), and DNA was isolated using QIAamp DNA Mini Kit. 50 ng of total DNA was subjected to quantitative PCR analysis as described above.

**Statistical analysis.** *In vitro* experiments were performed in triplicate on at least three independent occasions. *In vivo* experiments were performed with at least four animals per group. Analysis was by unpaired Student's *t*-test.

## SUPPLEMENTARY MATERIAL

**Figure S1.** CD46 expression in CD46 transgenic mice.

## ACKNOWLEDGMENTS

We thank Nicola Britton, Gregor Aitchison, and Angela McIlhoney for technical support, and the British Heart Foundation and Biotechnology and Biological Sciences Research Council for funding. S.N.W. is a recipient of the Philip Gray Fellowship from the Katharine Dormandy Trust.

## REFERENCES

1. Abbink, P, Lemckert, AA, Ewald, BA, Lynch, DM, Denholtz, M, Smits, S *et al.* (2007). Comparative seroprevalence and immunogenicity of six rare serotype recombinant adenovirus vaccine vectors from subgroups B and D. *J Virol* **81**: 4654–4663.
2. Sumida, SM, Truitt, DM, Lemckert, AA, Vogels, R, Custers, JH, Addo, MM *et al.* (2005). Neutralizing antibodies to adenovirus serotype 5 vaccine vectors are directed primarily against the adenovirus hexon protein. *J Immunol* **174**: 7179–7185.
3. Sprangers, MC, Lakhai, W, Koudstaal, W, Verhoeven, M, Koel, BF, Vogels, R *et al.* (2003). Quantifying adenovirus-neutralizing antibodies by luciferase transgene detection: addressing preexisting immunity to vaccine and gene therapy vectors. *J Clin Microbiol* **41**: 5046–5052.
4. Christ, M, Lusky, M, Stoeckel, F, Dreyer, D, Dieterlé, A, Michou, AI *et al.* (1997). Gene therapy with recombinant adenovirus vectors: evaluation of the host immune response. *Immunol Lett* **57**: 19–25.
5. Vogels, R, Zuidgeest, D, van Rijnsoever, R, Hartkoom, E, Damen, I, de Béthune, MP *et al.* (2003). Replication-deficient human adenovirus type 35 vectors for gene transfer and vaccination: efficient human cell infection and bypass of preexisting adenovirus immunity. *J Virol* **77**: 8263–8271.
6. Parker, AL, Waddington, SN, Buckley, SM, Custers, J, Havenga, MJ, van Rooijen, N *et al.* (2009). Effect of neutralizing sera on factor x-mediated adenovirus serotype 5 gene transfer. *J Virol* **83**: 479–483.
7. Parker, AL, Waddington, SN, Nicol, CG, Shayakhmetov, DM, Buckley, SM, Denby, L *et al.* (2006). Multiple vitamin K-dependent coagulation zymogens promote adenovirus-mediated gene delivery to hepatocytes. *Blood* **108**: 2554–2561.
8. Waddington, SN, Parker, AL, Havenga, M, Nicklin, SA, Buckley, SM, McVey, JH *et al.* (2007). Targeting of adenovirus serotype 5 (Ad5) and 5/47 pseudotyped vectors *in vivo*: fundamental involvement of coagulation factors and redundancy of CAR binding by Ad5. *J Virol* **81**: 9568–9571.
9. Waddington, SN, McVey, JH, Bhella, D, Parker, AL, Barker, K, Atoda, H *et al.* (2008). Adenovirus serotype 5 hexon mediates liver gene transfer. *Cell* **132**: 397–409.
10. Subr, V, Kostka, L, Selby-Millic, T, Fisher, K, Ulbrich, K, Seymour, LW *et al.* (2009). Coating of adenovirus type 5 with polymers containing quaternary amines prevents binding to blood components. *J Control Release* **135**: 152–158.
11. Nicol, CG, Graham, D, Miller, WH, White, SJ, Smith, TA, Nicklin, SA *et al.* (2004). Effect of adenovirus serotype 5 fiber and penton modifications on *in vivo* tropism in rats. *Mol Ther* **10**: 344–354.
12. Carlisle, RC, Di, Y, Cerny, AM, Sonnen, AF, Sim, RB, Green, NK *et al.* (2009). Human erythrocytes bind and inactivate type 5 adenovirus by presenting Coxsackie virus-adenovirus receptor and complement receptor 1. *Blood* **113**: 1909–1918.
13. Stone, D, Liu, Y, Shayakhmetov, D, Li, ZY, Ni, S and Lieber, A (2007). Adenovirus-platelet interaction in blood causes virus sequestration to the reticuloendothelial system of the liver. *J Virol* **81**: 4866–4871.
14. Hofherr, SE, Mok, H, Gushiken, FC, Lopez, JA and Barry, MA (2007). Polyethylene glycol modification of adenovirus reduces platelet activation, endothelial cell activation, and thrombocytopenia. *Hum Gene Ther* **18**: 837–848.
15. Raper, SE, Chirmule, N, Lee, FS, Wivel, NA, Bagg, A, Gao, GP *et al.* (2003). Fatal systemic inflammatory response syndrome in an ornithine transcarbamylase deficient patient following adenoviral gene transfer. *Mol Genet Metab* **80**: 148–158.
16. Bergelson, JM, Cunningham, JA, Droguett, G, Kurt-Jones, EA, Krithivas, A, Hong, JS *et al.* (1997). Isolation of a common receptor for Coxsackie B viruses and adenoviruses 2 and 5. *Science* **275**: 1320–1323.
17. Tomko, RP, Xu, R and Philipson, L (1997). HCAR and MCAR: the human and mouse cellular receptors for subgroup C adenoviruses and group B coxsackieviruses. *Proc Natl Acad Sci USA* **94**: 3352–3356.
18. Wickham, TJ, Mathias, P, Cheresch, DA and Nemerow, GR (1993). Integrins alpha v beta 3 and alpha v beta 5 promote adenovirus internalization but not virus attachment. *Cell* **73**: 309–319.
19. Nicklin, SA, Wu, E, Nemerow, GR and Baker, AH (2005). The influence of adenovirus fiber structure and function on vector development for gene therapy. *Mol Ther* **12**: 384–393.
20. Alemany, R and Curiel, DT (2001). CAR-binding ablation does not change biodistribution and toxicity of adenoviral vectors. *Gene Ther* **8**: 1347–1353.



21. Kalyuzhnyi, O, Di Paolo, NC, Silvestry, M, Hofherr, SE, Barry, MA, Stewart, PL *et al.* (2008). Adenovirus serotype 5 hexon is critical for virus infection of hepatocytes *in vivo*. *Proc Natl Acad Sci USA* **105**: 5483–5488.
22. Parker, AL, McVey, JH, Doctor, JH, Lopez-Franco, O, Waddington, SN, Havenga, MJ *et al.* (2007). Influence of coagulation factor zymogens on the infectivity of adenoviruses pseudotyped with fibers from subgroup D. *J Virol* **81**: 3627–3631.
23. Havenga, MJ, Lemckert, AA, Ophorst, OJ, van Meijer, M, Germeraad, WT, Grimbergen, J *et al.* (2002). Exploiting the natural diversity in adenovirus tropism for therapy and prevention of disease. *J Virol* **76**: 4612–4620.
24. Gaggar, A, Shayakhmetov, DM and Lieber, A (2003). CD46 is a cellular receptor for group B adenoviruses. *Nat Med* **9**: 1408–1412.
25. Havenga, MJ, Lemckert, AA, Grimbergen, JM, Vogels, R, Huisman, LG, Valerio, D *et al.* (2001). Improved adenovirus vectors for infection of cardiovascular tissues. *J Virol* **75**: 3335–3342.
26. Ni, S, Gaggar, A, Di Paolo, N, Li, ZY, Liu, Y, Strauss, R *et al.* (2006). Evaluation of adenovirus vectors containing serotype 35 fibers for tumor targeting. *Cancer Gene Ther* **13**: 1072–1081.
27. Kinugasa, N, Higashi, T, Nouse, K, Nakatsukasa, H, Kobayashi, Y, Ishizaki, M *et al.* (1999). Expression of membrane cofactor protein (MCP, CD46) in human liver diseases. *Br J Cancer* **80**: 1820–1825.
28. Murray, KP, Mathure, S, Kaul, R, Khan, S, Carson, LF, Twigg, LB *et al.* (2000). Expression of complement regulatory proteins-CD 35, CD 46, CD 55, and CD 59-in benign and malignant endometrial tissue. *Gynecol Oncol* **76**: 176–182.
29. Shayakhmetov, DM, Eberly, AM, Li, ZY and Lieber, A (2005). Deletion of penton RGD motifs affects the efficiency of both the internalization and the endosome escape of viral particles containing adenovirus serotype 5 or 35 fiber knobs. *J Virol* **79**: 1053–1061.
30. Shayakhmetov, DM, Li, ZY, Ni, S and Lieber, A (2004). Analysis of adenovirus sequestration in the liver, transduction of hepatic cells, and innate toxicity after injection of fiber-modified vectors. *J Virol* **78**: 5368–5381.
31. Wang, H, Liu, Y, Li, Z, Tuve, S, Stone, D, Kalyuzhnyi, O *et al.* (2008). *In vitro* and *in vivo* properties of adenovirus vectors with increased affinity to CD46. *J Virol* **82**: 10567–10579.
32. Brouwer, E, Havenga, MJ, Ophorst, O, de Leeuw, B, Gijssbers, L, Gillissen, G *et al.* (2007). Human adenovirus type 35 vector for gene therapy of brain cancer: improved transduction and bypass of pre-existing anti-vector immunity in cancer patients. *Cancer Gene Ther* **14**: 211–219.
33. DiPaolo, N, Ni, S, Gaggar, A, Strauss, R, Tuve, S, Li, ZY *et al.* (2006). Evaluation of adenovirus vectors containing serotype 35 fibers for vaccination. *Mol Ther* **13**: 756–765.
34. Sakurai, F, Mizuguchi, H, Yamaguchi, T and Hayakawa, T (2003). Characterization of *in vitro* and *in vivo* gene transfer properties of adenovirus serotype 35 vector. *Mol Ther* **8**: 813–821.
35. Shayakhmetov, DM, Li, ZY, Ni, S and Lieber, A (2002). Targeting of adenovirus vectors to tumor cells does not enable efficient transduction of breast cancer metastases. *Cancer Res* **62**: 1063–1068.
36. Shinozaki, K, Suominen, E, Carrick, F, Sauter, B, Kähäri, VM, Lieber, A *et al.* (2006). Efficient infection of tumor endothelial cells by a capsid-modified adenovirus. *Gene Ther* **13**: 52–59.
37. Stone, D, Liu, Y, Li, ZY, Tuve, S, Strauss, R and Lieber, A (2007). Comparison of adenoviruses from species B, C, E, and F after intravenous delivery. *Mol Ther* **15**: 2146–2153.
38. Tuve, S, Wang, H, Ware, C, Liu, Y, Gaggar, A, Bernt, K *et al.* (2006). A new group B adenovirus receptor is expressed at high levels on human stem and tumor cells. *J Virol* **80**: 12109–12120.
39. Inoue, N, Ikawa, M, Nakanishi, T, Matsumoto, M, Nomura, M, Seya, T *et al.* (2003). Disruption of mouse CD46 causes an accelerated spontaneous acrosome reaction in sperm. *Mol Cell Biol* **23**: 2614–2622.
40. Bernt, KM, Ni, S, Gaggar, A, Li, ZY, Shayakhmetov, DM and Lieber, A (2003). The effect of sequestration by nontarget tissues on anti-tumor efficacy of systemically applied, conditionally replicating adenovirus vectors. *Mol Ther* **8**: 746–755.
41. Baker, AH, McVey, JH, Waddington, SN, Di Paolo, NC and Shayakhmetov, DM (2007). The influence of blood on *in vivo* adenovirus bio-distribution and transduction. *Mol Ther* **15**: 1410–1416.
42. Sakurai, F (2008). Development and evaluation of a novel gene delivery vehicle composed of adenovirus serotype 35. *Biol Pharm Bull* **31**: 1819–1825.
43. Sakurai, F, Kawabata, K, Koizumi, N, Inoue, N, Okabe, M, Yamaguchi, T *et al.* (2006). Adenovirus serotype 35 vector-mediated transduction into human CD46-transgenic mice. *Gene Ther* **13**: 1118–1126.
44. Vigant, F, Descamps, D, Jullienne, B, Esselin, S, Connault, E, Opolon, P *et al.* (2008). Substitution of hexon hypervariable region 5 of adenovirus serotype 5 abrogates blood factor binding and limits gene transfer to liver. *Mol Ther* **16**: 1474–1480.
45. Miyazawa, N, Leopold, PL, Hackett, NR, Ferris, B, Worgall, S, Falck-Pedersen, E *et al.* (1999). Fiber swap between adenovirus subgroups B and C alters intracellular trafficking of adenovirus gene transfer vectors. *J Virol* **73**: 6056–6065.
46. Shayakhmetov, DM, Li, ZY, Ternovoi, V, Gaggar, A, Gharwan, H and Lieber, A (2003). The interaction between the fiber knob domain and the cellular attachment receptor determines the intracellular trafficking route of adenoviruses. *J Virol* **77**: 3712–3723.
47. Verhaagh, S, de Jong, E, Goudsmit, J, Lecollinet, S, Gillissen, G, de Vries, M *et al.* (2006). Human CD46-transgenic mice in studies involving replication-incompetent adenoviral type 35 vectors. *J Gen Virol* **87**(Pt 2): 255–265.
48. Tuve, S, Wang, H, Jacobs, JD, Yumul, RC, Smith, DF and Lieber, A (2008). Role of cellular heparan sulfate proteoglycans in infection of human adenovirus serotype 3 and 35. *PLoS Pathog* **4**: e1000189.
49. Atoda, H, Ishikawa, M, Mizuno, H and Morita, T (1998). Coagulation factor X-binding protein from Deinagkistrodon acutus venom is a Gla domain-binding protein. *Biochemistry* **37**: 17361–17370.
50. Adrian, M, Dubochet, J, Lepault, J and McDowell, AW (1984). Cryo-electron microscopy of viruses. *Nature* **308**: 32–36.